

Published in final edited form as:

Am J Hum Biol. 2011 ; 23(1): 22–28. doi:10.1002/ajhb.21135.

Biochemical specificity of von Economo neurons in hominoids

Cheryl D. Stimpson¹, Nicole A. Tetreault², John M. Allman², Bob Jacobs³, Camilla Butti⁴, Patrick R. Hof^{4,5}, and Chet C. Sherwood¹

¹Department of Anthropology, The George Washington University, Washington, DC 20052

²Division of Biology, California Institute of Technology, Pasadena, CA 91125

³Department of Psychology, The Colorado College, Colorado Springs, CO 80903

⁴Department of Neuroscience, Mount Sinai School of Medicine, New York, NY 10029

⁵New York Consortium in Evolutionary Primatology, New York, NY

Abstract

Von Economo neurons (VENs) are defined by their thin, elongated cell body and long dendrites projecting from apical and basal ends. These distinctive neurons are mostly present in anterior cingulate (ACC) and fronto-insular (FI) cortex, with particularly high densities in cetaceans, elephants, and hominoid primates (i.e., humans and apes). This distribution suggests that VENs contribute to specializations of neural circuits in species that share both large brain size and complex social cognition, possibly representing an adaptation to rapidly relay socially-relevant information over long distances across the brain. Recent evidence indicates that unique patterns of protein expression may also characterize VENs, particularly involving molecules that are known to regulate gut and immune function. In this study, we used quantitative stereologic methods to examine the expression of three such proteins that are localized in VENs – activating-transcription factor 3 (ATF3), interleukin 4 receptor (IL4R α) and neuromedin B (NMB). We quantified immunoreactivity against these proteins in different morphological classes of ACC layer V neurons of hominoids. Among the different neuron types analyzed (pyramidal, VEN, fork, enveloping, and other multipolar), VENs showed the greatest percentage that displayed immunostaining. Additionally, a higher proportion of VENs in humans were immunoreactive to ATF3, IL4R α , and NMB than in other apes. No other ACC layer V neuron type displayed a significant species difference in the percentage of immunoreactive neurons. These findings demonstrate that phylogenetic variation exists in the protein expression profile of VENs, suggesting that humans might have evolved biochemical specializations for enhanced interoceptive sensitivity.

Keywords

brain; evolution; ape; human; neuron

Introduction

Von Economo neurons (VENs) of the cerebral cortex are hypothesized to be centrally involved in the evolution of circuitry underlying self-awareness and social cognition (Nimchinsky et al., 1999; Allman et al., 2001; 2005; 2010). VENs were initially identified as morphologically distinct from pyramidal neurons by their thin, elongated cell body and long,

prominent dendrites projecting from apical and basal poles (Allman et al., 2005; Nimchinsky et al., 1995; von Economo, 1926). They are located predominantly in layer V of anterior cingulate (ACC) and fronto-insular cortex (FI), regions that are involved in the integration of interoception, emotion, and cognition. The relevance of this small population of neurons to social cognition is highlighted by the fact that VENs in FI are selectively and profoundly depleted in the behavioral variant of frontotemporal dementia, a neurodegenerative disease characterized by severe deficits in the patient's ability to recognize the emotional impact of their actions on others (Seeley et al., 2006, 2007). In addition, VENs have arisen several times among phylogenetically divergent species that share both large brain size and complex social organization, suggesting that they contribute to specializations of neural circuits that relay socially relevant information over long distances across the brain. Based on their morphology in Nissl-stained sections, high densities of VENs have been identified in ACC and FI of hominoid primates (Allman et al., 2005; Nimchinsky et al., 1995, 1999), cetaceans (Butti et al., 2009; Hof and Van der Gucht, 2007) and elephants (Hakeem et al., 2009).

Understanding the VENs' distinctive relationship to other cortical neuron types will shed light on their neurobiological function and contribution to cognitive adaptations. Watson et al. (2006) showed that in humans VENs have both fewer and shorter dendritic branches, as well as fewer dendritic spines, as compared to neighboring pyramidal neurons. These findings suggest that VENs are designed to perform relatively simple integrative functions within a narrow cortical column before conveying output to other brain regions for further processing. Additionally, VENs have significantly larger cell bodies than pyramidal neurons and express intense immunostaining against nonphosphorylated neurofilament protein (Nimchinsky et al., 1995), indicating that they carry large axons involved in the rapid conduction of information.

To further characterize the VENs, it is important to consider their biochemical phenotype. Allman et al. (2010) and Tetreault et al. (2010) reviewed a variety of proteins that are selectively expressed by VENs in humans and have a restricted distribution in layer V of ACC and FI. Among these proteins, activating transcription factor 3 (ATF3), the interleukin-4 receptor alpha chain (IL4R α), and neuromedin B (NMB) displayed some of the most intense staining in VENs.

ATF3 is a member of the mammalian activation transcription factor/cAMP responsive element-binding (CREB) protein family of transcription factors and its variants either activate or repress gene transcription from promoters of ATF binding elements. ATF3 has been shown to be involved in stress responses of the body (Chen et al., 1996; Hai et al., 1989) and the control of pain sensitivity in spinal cord neurons (Latremolier et al., 2008). The activity of ACC is closely related to the perceived unpleasantness of pain (Rainville et al., 1998), and thus the expression of ATF3 in the VENs might be related to the regulation of pain sensitivity in this structure as well.

IL4R α is a type I cytokine receptor which binds interleukin-4 and interleukin-13 to regulate the production of immunoglobulin E (IgE), thus playing a crucial role in allergic reactions, particularly asthma (Wenzel et al., 2007). In the brain, IL4R α plays an important role in inflammatory reactions and has been implicated in the pathology of schizophrenia (Nawa et al., 2000; 2006; Watanabe et al., 2008). Anterior cingulate cortex is involved in the regulation of the severity of asthmatic responses to allergens in human subjects (Rosenkranz and Davidson, 2009) and IL4R α expression in the VENs may participate in this process.

NMB is a peptide that is involved in the release of digestive enzymes in the stomach, in smooth muscle contractions during intestinal peristalsis, in the mounting of immune

responses to potentially damaging ingested substances, and in the control of appetite by the brain (Jensen et al., 2008). NMB participates in the local control of the intestinal tract, but also functions at higher levels of gut control, first in the hypothalamus where the digestive processes are integrated with other homeostatic systems of the body, and second in the insular and related cortices, where gut feelings and the control of the gut interact with circuitry activated in awareness, motivation and conscious decision-making (Allman et al., 2010). The high level of expression of proteins that are involved in immune response and digestion by VENs suggests their role in monitoring of a “body-loop” that incorporates visceral states and emotions in the awareness of self and others (Damasio, 1994; Allman et al., 2010).

In the present study, we examined whether ATF3, IL4R α , and NMB display selective distributions among the various neuron types in layer V of the ACC of hominoid primates (i.e., humans and apes) to test the hypothesis that these proteins serve a special role in the biochemical function of VENs.

Materials and Methods

Specimens

Formalin-fixed brain samples were obtained from hominoid primates, including *Homo sapiens* (n = 6), *Pan troglodytes* (n = 5), *Pan paniscus* (n = 1), *Gorilla gorilla* (n = 5), *Pongo pygmaeus* (n = 5), *Hylobates muelleri* (n = 1), and *Symphalangus syndactylus* (n = 1). Table 1 provides details about age at death and the sex of subjects used in this study. Nonhuman brains came from animals that were housed at various zoological and research facilities according to each institution's guidelines; the nonhuman primate subjects were not part of any research protocol that may have contributed to their death. Human brain samples were provided by the El Paso County coroner's office in Colorado. None of the humans showed evidence of neurological or psychiatric dysfunction prior to death and all postmortem brains appeared normal upon routine neuropathology evaluation.

Tissue preparation and immunohistochemistry

Within 19 hours of each subject's death, the brain was removed and immersed in 10% formalin. In most cases, the brain was transferred to 0.1M phosphate buffered saline (PBS) with 0.1% sodium azide solution after 10 days and stored at 4° C. Tissue blocks, which included the left anterior cingulate cortex (Brodmann's area 24) were cryoprotected by immersion in buffered sucrose solutions up to 30%, embedded in Tissue-Tek medium, frozen in a slur of dry ice and isopentane, and sectioned at 40 μ m with a sliding microtome in the coronal plane.

Free-floating sections were stained with rabbit polyclonal IgG₁ antibodies against a peptide mapping to the C-terminus of human ATF3 (1:100 dilution, sc-188, Santa Cruz Biotechnology, Santa Cruz, CA), an epitope on the C-terminal cytoplasmic domain of human IL4R α (1:100 dilution, sc-684, Santa Cruz Biotechnology), and a fusion protein to NMB, which is recognized as a band at 13kD by Western blot (1:100 dilution, 10888-1-AP, ProteinTech Group, Chicago, IL). Prior to immunostaining, sections were rinsed thoroughly in PBS and pretreated for antigen retrieval by incubation in 10 mM sodium citrate buffer (pH 3.5) at 37° C in an oven for 30 minutes. Sections were then rinsed and immersed in a solution of 0.75% hydrogen peroxide in 75% methanol to eliminate endogenous peroxidase activity. After rinsing again, sections were incubated in the primary antibody diluted in PBS with 2% normal horse serum and 0.1% Triton X-100 detergent for approximately 24 hours on a rotator at 4° C. After rinsing in PBS, sections were incubated in biotinylated anti-rabbit IgG (1:200 dilution, BA-2000, Vector Laboratories, Burlingame, CA) and processed with

the avidin-biotin-peroxidase method using a Vectastain Elite ABC kit (pk-6100, Vector Laboratories). Sections were rinsed again in PBS, followed by a rinse in sodium acetate buffer. Immunoreactivity was revealed using 3,3'-diaminobenzidine and nickel enhancement according to a modification of the methods in Shu et al. (1988) (Van der Gucht et al., 2001). Specificity of the reaction was confirmed by processing negative control sections as described, excluding the primary antibody. No immunostaining was observed in control sections.

Stereologic analyses

Stereology was performed to determine whether different morphological classes of neurons in layer V of ACC showed variation in their expression of ATF3, IL4R α , and NMB across species. To examine this question, we used stereologic principles to obtain estimates of the density of immunoreactive neurons in layer V, as well as the total population of Nissl-stained neurons from adjacent sections (see Sherwood et al., 2007).

Quantification of the numerical density of ATF3-immunoreactive (-ir), IL4R α -ir, and NMB-ir neurons in layer V was performed using a Zeiss Axioplan 2 photomicroscope (Zeiss, Thornwood, NY) equipped with a Ludl XY motorized stage (Ludl Electronics, Hawthorne, NY), Heidenhain z-axis encoder, and an Optronics MicroFire color videocamera (Optronics, Golenta, CA) coupled to a Dell PC workstation running StereoInvestigator software (MBF Bioscience, Williston, VT). Beginning at a random starting point, three equidistantly spaced sections were chosen for stereologic analysis. To quantify the density of different immunoreactive neuron classes, we outlined the boundaries of layer V in ACC at low magnification and placed a set of optical disector frames ($100 \times 100 \mu\text{m}$) with a scan grid size of $100 \times 100 \mu\text{m}$ to sample the region of interest exhaustively. Disector analysis was performed under Koehler illumination using a $63\times$ objective (Zeiss Plan-Apochromat, N.A. 1.4). The thickness of optical dissectors was set to $8 \mu\text{m}$, with a $1\text{-}\mu\text{m}$ guard zone at the top of the section. Adjacent Nissl-stained sections were also quantified to provide the total density of each morphological class as a frame of reference for comparison to those characterized by immunoreactivity. To estimate the density of neurons in layer V from Nissl-stained sections, we used a disector frame size of $30 \times 30 \mu\text{m}$ and $6 \mu\text{m}$ -thick optical dissectors that were placed in a systematic random fashion using a 100×100 scan grid. Using this strategy, in each subject we sampled an average of 162 ± 77 (s.d.) Nissl-stained neurons, 141 ± 96 ATF3-ir neurons, 196 ± 101 IL4R α -ir neurons, and 159 ± 101 NMB-ir neurons. All numerical densities of neurons derived from these optical disector counts were corrected by the number-weighted mean section thickness as described in Sherwood et al. (2007).

In both immunostained and Nissl-stained sections, we categorized each neuron that was encountered within the permitted boundaries of optical disector frames into one of five different classes based on its morphology. The five categories included: (1) pyramidal, (2) VEN, (3) fork neuron, (4) enveloping neuron, and (5) other multipolar (Fig. 1). Pyramidal neurons were identified by their large, triangular-shaped cell body, a singular, large apical dendrite and multiple large basal dendrites that branched away from the soma. VENs were identified as previously described (Nimchinsky et al., 1995,1999), with a large, thin cell body and single, thick apical and basal dendrites. Fork neurons have been previously described in the human insular cortex by Ngowyang (1932). They are similar to VENs in their basal aspect with a single large tapered dendrite, but they are distinguished by two apical dendrites that bifurcate close to the soma and project towards layer I in a Y-like fashion. Previously, "enveloping cells" have been described by both de Crinis (1934) and Syring (1957). We recognized "enveloping neurons" as a type that was commonly observed abutting capillaries or other cells. Either their soma or dendrite would "hug" the space created by a capillary. The category "other" included neurons that did not meet the criteria for any other cell morphology described above, but were positively identified as neurons

based on cell body and dendrites. Often, these would include neurons with either non-pyramidal or non-circular cell bodies or dendrites projecting out at varying angles and locations on the soma. Staining intensity varied among individuals, therefore neurons were quantified when they were several shades darker than the background, the shape of the soma was easily identified and major dendrites were clearly projecting from the cell body.

We examined inter-rater reliability in the identification and quantification of these different morphological classes by choosing six cases for analysis by a second rater (CCS) who was blind to the results of the primary rater (CDS). The second rater used the stereologic design described above to estimate the density of different morphological classes of neurons in layer V from three cases that were immunostained against ATF3 and three cases that were immunostained against NMB (i.e., a total of 30 neuron types were analyzed). The intraclass correlation coefficient for neuronal density values between raters was 0.98 ($P > 0.001$), indicating a very high degree of agreement.

Statistical significance was adjusted for multiple tests for each hypothesis that was examined.

Results

Specificity of immunostaining to different morphological types of neurons in layer V

We observed immunostaining against ATF3, IL4R α , and NMB in ACC of all hominoid species under investigation (Fig. 2). As previously described in humans (Tetreault et al., 2010), neurons in layer V showed the most intense immunoreactivity to these proteins. Across all species, the predominant type of neuron in layer V that expressed immunoreactivity to ATF3, IL4R α , and NMB had a pyramidal morphology (Kruskal-Wallis tests, all comparisons $P < 0.001$; Fig. 3a). On average in hominoids, pyramidal-shaped cells represented 81% of all ATF3-ir neurons, 83% of IL4R α -ir neurons, and 82% of NMB-ir neurons.

We used the total density of each morphological class from adjacent Nissl-stained sections to calculate a ratio representing the percent of the total neuron population that expressed immunoreactivity for each protein. In the pooled sample of hominoids, a higher percentage of VENs displayed immunoreactivity for each of the proteins as compared with all other morphological classes of layer V neurons (Fig. 3b). Results of Kruskal-Wallis tests are shown in Table 2.

Phylogenetic variation in immunostaining

Multivariate analysis of variance (MANOVA) was used to test whether phylogenetic groups differed in the percentage of neurons within each morphological class that expressed immunoreactivity to ATF3, IL4R α , and NMB (Fig. 4). For this analysis, species were used as groups; we pooled hylobatids – *Hylobates muelleri* ($n = 1$) and *Symphalangus syndactylus* ($n = 1$) – and the genus *Pan* – *Pan troglodytes* ($n = 5$) and *Pan paniscus* ($n = 1$) – because of limited sample sizes.

The MANOVA revealed a significant overall effect for ATF3 (Wilks $\Lambda = 0.171$, $F = 1.785$, $P = 0.049$, $df = 20$). Of the five morphological classes of neurons, only VENs displayed a significant between-group effect (Kruskal-Wallis test statistic = 12.571, $P = 0.014$, $df = 4$). Follow-up pair-wise tests indicated that a significantly greater percentage of VENs in *Homo* were immunoreactive for ATF3 than in *Pan* ($P = 0.033$) and *Pongo* ($P = 0.022$). On average, 31% of VENs expressed ATF3 in humans, whereas 12% of VENs were immunoreactive in the other apes.

Similarly, the MANOVA was significant for IL4R α (Wilks $\Lambda = 0.132$, $F = 2.137$, $P = 0.015$, $df = 20$) and the VENs were the only neuron class that showed significant phylogenetic variation (Kruskal-Wallis test statistic = 13.451, $P = 0.009$, $df = 4$). *Homo* had a significantly greater percentage of IL4R α -immunoreactive VENs than *Pan* ($P = 0.09$), *Gorilla* ($P = 0.01$), and *Pongo* ($P = 0.01$). On average, 66% of VENs expressed IL4R α in humans, whereas 20% of VENs were immunoreactive in the other apes.

In contrast, the MANOVA did not reveal any phylogenetic effects for the percentage of neurons that were immunoreactive to NMB (Wilks Lambda = 0.198, $F = 1.596$, $P = 0.091$, $df = 20$), although it is notable that a higher percentage of VENs in humans were immunoreactive to NMB relative to the other apes. Across all hominoids, a mean of 22% of VENs were immunoreactive for NMB.

Discussion

VENs have emerged multiple times within ACC and insular cortex in mammalian phylogeny, occurring in large-brained, social animals, such as hominoid primates (Allman et al., 2005; Nimchinsky et al., 1995, 1999), cetaceans (Butti et al., 2009; Hof and Van der Gucht, 2007) and elephants (Hakeem et al., 2009). Previous research has demonstrated the morphological distinctiveness of VENs (Watson et al., 2006), described their distribution in different species (Allman et al., 2010; Butti et al., 2009; Hakeem et al., 2009; Nimchinsky et al., 1999), and surveyed their protein expression profile (Allman et al., 2010; Tetreault et al., 2010). The current results provide the first quantitative analysis of phylogenetic variation in the biochemical phenotype of VENs relative to other layer V neurons in hominoid primates. Our findings indicate that ATF3, IL4R α , and NMB proteins are expressed in a large proportion of VENs in the ACC of hominoids, whereas other neuron classes show immunoreactivity to these proteins at a lower frequency. This suggests that these pain-, immune- and digestion-related proteins may perform a specific function in regulating the physiological responses of VENs.

We also found that, among all the morphological classes of neurons in layer V of ACC, only VENs exhibited a difference among species in the proportion of neurons that were immunoreactive to these markers. Notably, humans had a significantly greater percentage of VENs that were immunoreactive to ATF3 and IL4R α as compared to other apes. This pattern indicates that specializations of VENs may evolve along multiple routes, including modifications of morphology, distributions, and biochemical phenotype.

ATF3, IL4R α and NMB are all hypothesized to be involved in aspects of visceral monitoring that might be relevant to social cognition (Allman et al., 2010; Bédard et al., 2007; Chen et al., 1996; Hai et al., 1989; Nawa et al., 2000; Ohki-Hamazaki, 2000; Tetreault et al., 2010). The biochemical characteristics of VENs that distinguish them from other neurons may contribute to self-awareness of body states such as the regulation of pain sensitivity, immune functioning, visceral activity, and appetite. Such increased neural interoception of one's own homeostatic condition may be used as a reference in the evaluation of social partners' emotions during interactions (Craig, 2009). We speculate that such adaptations would be particularly significant in species such as hominoids, as well as cetaceans and elephants (Connor, 2007), where fission-fusion social organization and the maintenance of alliances might have favored the evolution of enhanced capacities in social cognition (Potts, 2004; Lusseau, 2007).

Interestingly, ATF3 and IL4R α were expressed in a significantly higher proportion of VENs among humans as compared to other apes. NMB immunoreactivity was also found in a higher percentage of VENs in humans, although this difference did not reach statistical

significance. ATF3 may modulate the emotional salience of pain experienced by oneself and others (empathy). Anterior cingulate cortex and the anterior insula (including FI) are strongly implicated in the neurobiological processes of empathy (Singer et al, 2004). IL4R α regulates the balance of self-protective and allergic responses, and its expression in the VENs is consistent with the role of ACC in the regulation of the severity of asthmatic responses to allergens (Rosenkranz and Davidson, 2009). Also of note, an imbalance of IL4R α protein and associated decreases in T cells are observed in patients with schizophrenia, a psychiatric disorder in humans that leads to a deficit of verbal cognition, social emotion and logical construction (Nawa et al., 2006). Taken together, these findings suggest that these proteins may perform an important role in regulating signals relevant to social awareness.

We have demonstrated that certain biochemical characteristics of VENs distinguish them from other layer V neurons in ACC of hominoids, with humans showing the highest percentages of VENs that are immunoreactive to ATF3, IL4R α , and NMB. Such modifications of VENs, which are critically situated in ACC and FI circuits, may be associated with an increased capacity for social intelligence through enhanced monitoring of one's own physiological states. Given the independent evolution of the VEN morphology in other large-brained species, such as whales and elephants, future studies may test the hypothesis that these unique neurons show a similar biochemical phenotype in these distantly related taxa.

Acknowledgments

We thank Drs. Kebreten Manaye, William Seeley, Bud Craig, and Joseph Erwin for helpful discussion related to this research. Non-human brain materials used in this study were loaned by the Great Ape Aging Project (NIH grant AG14308), the Foundation for Comparative and Conservation Biology, and the Cleveland Metroparks Zoo. This work was supported by the National Science Foundation (BCS-0515484, BCS-0549117, BCS-0827531, DGE-0801634), the National Institutes of Health (NS42867), and the James S. McDonnell Foundation (22002078).

References

- Allman JM, Hakeem A, Erwin JM, Nimchinsky E, Hof PR. The anterior cingulate cortex: the evolution of an interface between emotion and cognition. *Annals of the New York Academy of Sciences*. 2001; 935:107–117. [PubMed: 11411161]
- Allman JM, Watson KK, Tetreault NA, Hakeem AY. Intuition and autism: a possible role for von Economo neurons. *Trends in Cognitive Sciences*. 2005; 9:367–373. [PubMed: 16002323]
- Allman JM, Tetreault NA, Hakeem AY, Manaye KF, Semendeferi K, Erwin JM, Park S, Goubert V, Hof PR. The von Economo neurons in fronto-insular and anterior cingulate cortex in great apes and humans. *Brain Structure & Function*. 2010; 214:495–517. [PubMed: 20512377]
- Bédard T, Mountney C, Kent P, Anisman H, Merali Z. Role of gastrin-releasing peptide and neuromedin B anxiety and fear-related behavior. *Behavioural Brain Research*. 2007; 179:133–140. [PubMed: 17335915]
- Butti C, Sherwood CC, Hakeem AY, Allman JM, Hof PR. Total number and volume of von Economo neurons in the cerebral cortex of Cetaceans. *The Journal of Comparative Neurology*. 2009; 515:243–259. [PubMed: 19412956]
- Chen BPC, Wolfgang CD, Hai T. Analysis of ATF3, a transcription factor induced by physiological stresses and modulated by gadd153/Chop10. *Molecular and Cellular Biology*. 1996; 16:1157–1168. [PubMed: 8622660]
- Connor RC. Dolphin social intelligence: complex alliance relationships in bottlenose dolphins and a consideration of selective environments for extreme brain size evolution in mammals. *Philosophical Transactions of the Royal Society B*. 2007; 362:587–602.
- Craig AD. How do you feel? Interoception: the sense of the physiological condition of the body. *Nature Reviews*. 2002; 3:655–666.

- Craig AD. How do you feel - now? The anterior insula and human awareness. *Nature Reviews*. 2009; 10:59–70.
- de Crinis M. Über die Spezialzellen in der menschlichen Grosshirnrinde. *J Psych Neurol*. 1934; 45:439–449.
- Damasio, AR. *Descartes' Error*. Pan Macmillan; 1994.
- Hai T, Liu F, Coukos WJ, Green MR. Transcription factor ATF cDNA clones: an extensive family of leucine zipper proteins able to selectively form DNA-binding heterodimers. *Genes and Development*. 1989; 3:2083–2090. [PubMed: 2516827]
- Hakeem AY, Sherwood CC, Bonar CJ, Butti C, Hof PR, Allman JM. Von Economo neurons in the elephant brain. *The Anatomical Record*. 2009; 292:242–248. [PubMed: 19089889]
- Hof PR, Van der Gucht E. Structure of the cerebral cortex of the humpback whale, *Megaptera novaeangliae* (Cetacea, Mysticeti, Balaenopteridae). *The Anatomical Record*. 2007; 290:1–31. [PubMed: 17441195]
- Jensen R, Battey J, Spindel R, Benya R. Mammalian bombesin receptors: nomenclature, distribution, pharmacology, signaling, and functions in normal and disease states. *Pharmacol.Rev*. 2008; 60:1–42. [PubMed: 18055507]
- Latremolier A, Mauborgne A, Masson J, Bourgoin S, Kayser V, Hamon M, Pohl M. Differential implications of proinflammatory cytokine interleukin-6 in the development of cephalic versus extracephalic neuropathic pain in rats. *Journal of Neuroscience*. 2008; 28:8489–8501. [PubMed: 18716207]
- Lusseau D. Evidence for social role in a dolphin social network. *Evolutionary Ecology*. 2007; 21:357–366.
- Mosmann TR, Cherwinski H, Bond MW, Giedlin MA, Coffman RL. Two types of murine helper T cell clone. *The Journal of Immunology*. 1986; 136:2348–2357. [PubMed: 2419430]
- Nawa H, Takahashi M, Patterson PH. Cytokine and growth factor involvement in schizophrenia - support for the developmental model. *Molecular Psychiatry*. 2000; 5:594–603. [PubMed: 11126390]
- Nawa H, Takei N. Recent progress in animal modeling of immune inflammatory processes in schizophrenia: implication of specific cytokines. *Neuroscience Research*. 2006; 56:2–13. [PubMed: 16837094]
- Ngoyang G. Beschreibung einer art von spezialzellen in der inselrinde. *Journal of Psychological Neurology*. 1932; 44:671–674.
- Nimchinsky EA, Vogt BA, Morrison JH, Hof PR. Spindle neurons of the human anterior cingulate cortex. *The Journal of Comparative Neurology*. 1995; 355:27–37. [PubMed: 7636011]
- Nimchinsky EA, Gillissen E, Allman JM, Perl DP, Erwin JM, Hof PR. A neuronal morphologic type unique to humans and great apes. *Proceedings of the National Academy of Sciences*. 1999; 96:5268–5273.
- Ohki-Hamazaki H. Neuromedin B. *Progress in Neurobiology*. 2000; 62:297–312. [PubMed: 10840151]
- Potts R. Paleoenvironmental basis of cognitive evolution in great apes. *American Journal of Primatology*. 2004; 62:209–28. [PubMed: 15027093]
- Rainville P, Duncan G, Price D, Carrier B, Bushnell C. Pain affect encoded in human anterior cingulate but not somatosensory cortex. *Science*. 1998; 277:968–971. [PubMed: 9252330]
- Rosenkranz M, Davidson R. Affective circuitry and the mind-body influences in asthma. *Neuroimage*. 2009; 47:972–980. [PubMed: 19465136]
- Seeley WW, Carlin DA, Allman JM, Macedo MN, Bush C, Miller BL, DeArmond SJ. Early frontotemporal dementia targets neurons unique to apes and humans. *Annals of Neurology*. 2006; 60:660–667. [PubMed: 17187353]
- Seeley WW, Allman JM, Carlin DA, Crawford RK, Macedo MN, Greicius MD, DeArmond SJ, Miller BL. Divergent social functioning in the behavioral variant frontotemporal dementia and Alzheimer Disease: reciprocal networks and neuronal evolution. *Alzheimer Disease and Associated Disorders*. 2007; 12:S50–S57. [PubMed: 18090425]

- Sherwood CC, Raghanti MA, Stimpson CD, Bonar CJ, de Sousa AA, Preuss TM, Hof PR. Scaling of inhibitory interneurons in areas V1 and V2 of anthropoid primates as revealed by calcium-binding protein immunohistochemistry. *Brain, Behavior and Evolution*. 2007; 69:176–195.
- Shu S, Ju G, Fan L. The glucose oxidase-DAB-nickel method in peroxidase histochemistry of the nervous system. *Neuroscience Letters*. 1989; 85:169–171. [PubMed: 3374833]
- Silani G, Bird G, Brindley R, Singer T, Frith C, Frith U. Levels of emotional awareness and autism: an fMRI study. *Social Neuroscience*. 2008; 3:97–112. [PubMed: 18633852]
- Singer T, Seymour B, O'Doherty J, Kaube H, Dolan R, Frith C. Empathy for pain involves the affective but not sensory components of pain. *Science*. 2004; 303:1157–1162. [PubMed: 14976305]
- Syring A. Die verbreitung von spezialzellen in der grosshirnrinde verschiedener säugetiergruppen. *Cell and Tissue Research*. 1957; 45:399–434. [PubMed: 13434321]
- Tetreault, NA.; Hakeem, AY.; Stimpson, CD.; Jacobs, B.; Sherwood, CC.; Allman, JM. 2010 Neuroscience Meeting Planner. Society for Neuroscience; San Diego, CA: 2010. Immune regulation and the role of Von Economo neurons and fork cells in human frontoinsular and anterior cingulate cortex. Program No. 403.7.. Online
- Van der Gucht E, Vandesande F, Arckens L. Neurofilament protein: a selective marker for the architectonic parcellation of the visual cortex in the adult cat brain. *Journal of Comparative Neurology*. 2001; 441:345–368. [PubMed: 11745654]
- von Economo C. Eine neue Art Spezialzellen des Lobus cinguli and Lobus insulae. *Zschr ges Neurology and Psychiatry*. 1926; 100:706–712.
- Watanabe Y, Nunokawa A, Shibuya M, Kaneko N, Nawa H, Someya T. Association study of interleukin 2 (IL2) and IL4 with schizophrenia in a Japanese population. *European Archives of Psychiatry and Clinical Neuroscience*. 2008; 258:422–427. [PubMed: 18574615]
- Watson KK, Jones TK, Allman JM. Dendritic architecture of the von Economo neuron. *Neuroscience*. 2006; 141:1107–1112. [PubMed: 16797136]
- Wenzel S, Balzar S, Ampleford E, Hawkins G, Busse W, Calhoun W, Castro M, Chung K, Erzurum S, Gaston B, Israel E, Teague W, Curran-Everett D, Meyers D, Bleecker E. IL4Ra mutations are associated with asthma exacerbations and mast cell/IgE expression. *Am J Respir Crit Care Med*. 2007; 175:570–576. [PubMed: 17170387]

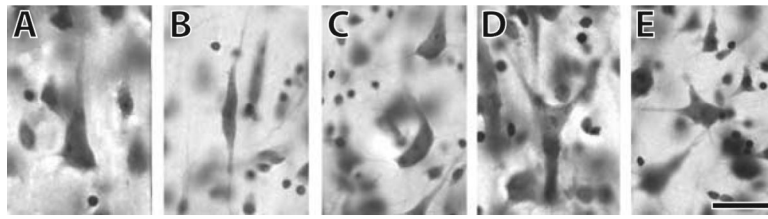


Figure 1. Nissl stain illustrating different morphological classes of neurons analyzed in this study found in layer V of anterior cingulate cortex. A) a pyramidal neuron from a gorilla; B) a VEN from a human; C) an enveloping neuron from a human; D) a fork neuron from a bonobo; and E) a neuron that was classified as “other” from a human. Scale bar is 20 μ m. Each morphological class was counted separately in stereologic analyses.

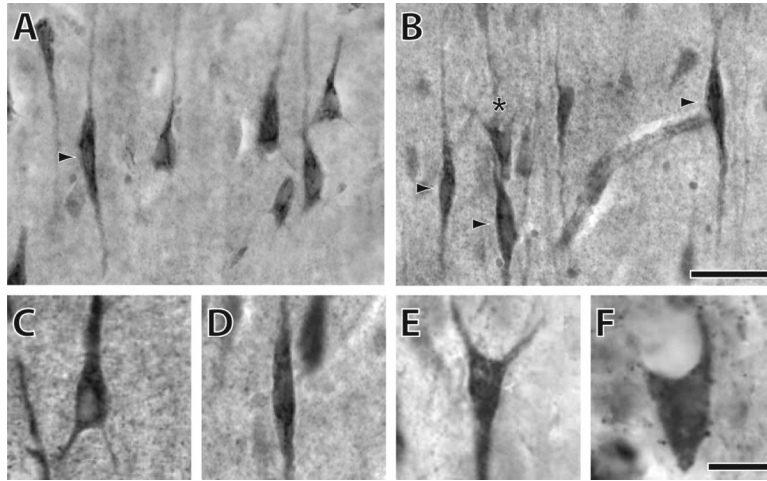


Figure 2.

Immunostaining of ATF3, IL4R α , and NMB in anterior cingulate cortex of various hominoids. A) IL4R α immunostaining in a human illustrating several pyramidal neurons and a VEN as indicated by the arrow; B) IL4R α immunostaining in a human illustrating several VENs (arrow) and a fork neuron (asterisk); C) ATF3 immunostaining of a pyramidal neuron from a human; D) IL4R α immunostaining of a VEN from a chimpanzee; E) IL4R α immunostaining of a fork neuron from an orang-utan; F) NMB immunostaining of an enveloping neuron from a siamang. The scale bar in panels A and B is 40 μ m. The scale bar in panels C-F is 10 μ m.

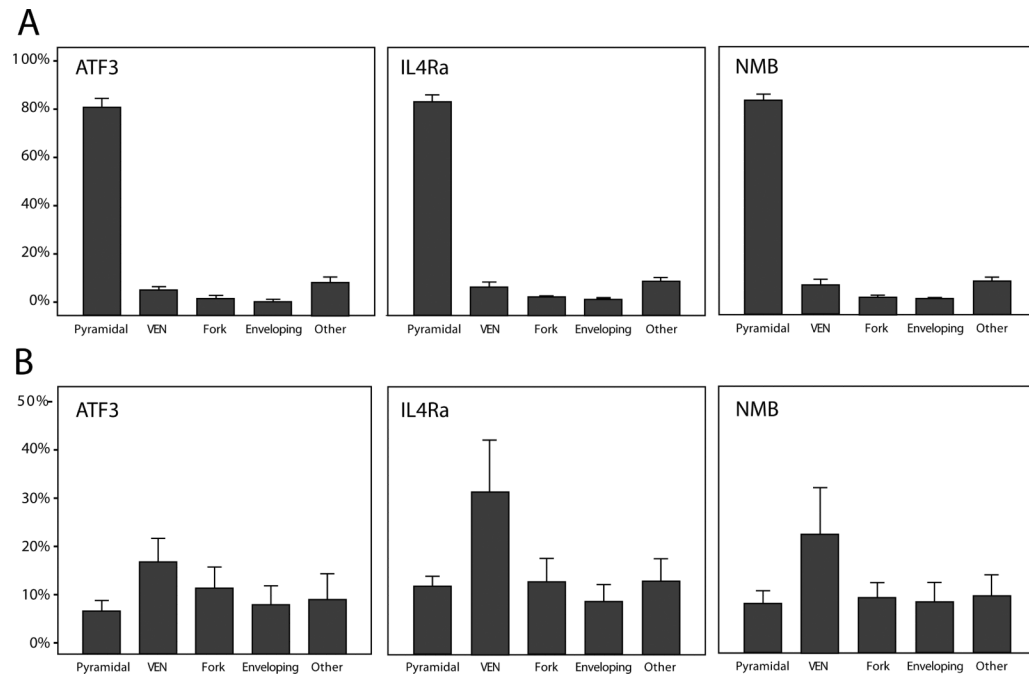


Figure 3.

Distribution of neuron types according to immunoreactivity in layer V of anterior cingulate cortex across all hominoids. (A) The percentage of immunoreactive neurons for each protein from each morphological type. (B) The percentage of immunoreactive neurons out of the total number of Nissl-stained neurons for each protein and each neuron type. Bar indicates mean; error bars indicate 2 standard errors.

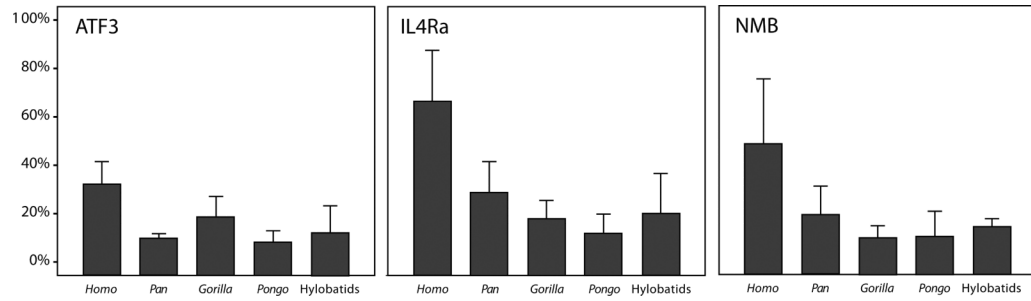


Figure 4. Percentage of immunoreactive VENs out of the total Nissl-stained neuron population in different species. Bar indicates mean; error bars indicate 2 standard errors.

Table 1

Subjects used in this study

Species	Sex	Age (years)
<i>Hylobates muelleri</i>	M	19
<i>Symphalangus syndactylus</i>	M	33
<i>Pongo pygmaeus</i>	F	31
<i>Pongo pygmaeus</i>	F	23
<i>Pongo pygmaeus</i>	M	39
<i>Pongo pygmaeus</i>	M	33
<i>Pongo pygmaeus</i>	M	11
<i>Gorilla gorilla</i>	F	50
<i>Gorilla gorilla</i>	M	49
<i>Gorilla gorilla</i>	M	43
<i>Gorilla gorilla</i>	M	21
<i>Gorilla gorilla</i>	M	13
<i>Pan paniscus</i>	F	25
<i>Pan troglodytes</i>	F	41
<i>Pan troglodytes</i>	F	27
<i>Pan troglodytes</i>	F	19
<i>Pan troglodytes</i>	M	41
<i>Pan troglodytes</i>	M	40
<i>Homo sapiens</i>	F	48
<i>Homo sapiens</i>	F	25
<i>Homo sapiens</i>	F	22
<i>Homo sapiens</i>	M	64
<i>Homo sapiens</i>	M	50
<i>Homo sapiens</i>	M	44

Table 2

Results of Kruskal-Wallis tests for differences in the percentage of immunoreactive cells among neuron types in the pooled hominoid sample

Protein	Test statistic	df	<i>P</i>	Neuron types that show a significant pair-wise differences from VENs (adjusted <i>P</i> < 0.05)
ATF3	16.87	4	0.002	pyramidal, enveloping, other
IL4R α	20.04	4	0.000	fork, enveloping, other
NMB	12.85	4	0.012	enveloping